Generation and detection of terahertz radiation with multilayered electro-optic polymer films

Alexander M. Sinyukov and L. Michael Hayden

Department of Physics, University of Maryland, Baltimore County, 1000 Hilltop Circle, Baltimore, Maryland 21250

Received June 22, 2001

We use optical rectification and electro-optic sensing to generate and detect terahertz radiation, using individual and multilayered stacks of electro-optic polymer films. For comparable thickness, the polymer films are more efficient generators and detectors of terahertz radiation than ZnTe crystals. © 2002 Optical Society of America

OCIS codes: 190.7110, 190.4710.

Terahertz (THz) imaging and spectroscopy have the potential for widespread application in electronic device inspection,[1] medical diagnostics,[2] and materials science.[3] Wide-bandwidth, highly efficient sources and detectors must be developed if the full potential of these THz applications is to be realized.

The two main methods in use today for generation and detection of wideband THz radiation utilize photoconducting dipole antennas or electro-optic (EO) materials. Of the two methods, conventional photoconducting dipole antennas have superior sensitivity but have a limited bandwidth of ~7 THz.[4] Although recent reports of detection of 60 THz in low-temperature GaAs photoconducting dipole antennas have been made,[5] useful signal-to-noise ratios and high-frequency roll-off may limit their use in mid-IR spectroscopic applications. In addition, the peak-to-peak low-temperature GaAs signal was only 1/20th of that obtained from ZnTe.[6] EO crystals of ZnTe have shown high-frequency performance up to 30 THz,[7] and the organic crystal DAST has shown performance up to 20 THz.[8] However, both of these EO crystals exhibit wide gaps in their frequency responses that are due to absorption from lattice vibrations and to a phase mismatch between the THz beam and the probe beam in the EO sensor. Tunable high-frequency THz output up to 41 THz has been reported in crystals of GaSe,[9] although in that case the bandwidth was only 10–15 THz about any chosen center frequency.

For taking advantage of the wide-bandwidth radiation available from ultrashort laser pulses (10 fs–100 THz), materials with instantaneous responses based on nonresonant second-order optical nonlinearities are useful.[10] Such materials include inorganic EO crystals,[11–13] organic crystals,[8,14] and EO polymers.[15,16] Because of its good phase-matching properties and reasonable EO coefficient, the most popular EO material for THz generation and detection is the inorganic crystal ZnTe. This crystal has the EO coefficient $r_{41} \sim 4$ pm/V. In contrast, EO polymers with $r_{33} > 120$ pm/V have been reported.[17] Large EO coefficients are not a guarantee of quadratic scaling of the emitted THz power, however. The organic crystal DAST has $r_{11} \sim 77$ pm/V at 800 nm,[18] yet it shows a subquadratic enhancement of THz power compared with ZnTe (Refs. 8 and 14) as a result of crystal imperfections and surface irregularities. In addition, the frequency response of DAST crystals shows large gaps that are due to phonon absorption and a large phase mismatch.[8] Finally, because of large dispersion in $\chi^{(2)}$, r_{11} is only ~48 pm/V at 1.5 μm in DAST, whereas $r_{33} \sim 60$ pm/V has been reported in amorphous EO polymers at 1.5 μm.[19]

EO polymers have low dielectric constants in the THz regime, leading to better phase matching between the phase velocity of the THz wave front and the group velocity of the optical pulse. Nahata *et al.*[15] measured the index and absorption of a methyl methacrylate EO polymer from 0.2 to 1 THz and found a nearly constant index of ~1.75 and an absorption of only ~4 cm^{-1}. We can use this index at THz frequencies with an optical group index of ~1.78 for our composites to estimate the group-velocity mismatch and hence the coherence length.[10,20] $l_c = \pi/\Delta k = \pi/[\omega_{\mathrm{THz}}|n_{\mathrm{opt}} - \lambda_{\mathrm{opt}}(\mathrm{d}n_{\mathrm{opt}}/\mathrm{d}\lambda)_{\lambda_{\mathrm{opt}}} - n_{\mathrm{THz}}|]$. We estimate that our composites will have coherence lengths of $l_c \sim 5$ mm at 1 THz. If we neglect dispersion, ZnTe and DAST have coherence lengths of $l_c \sim 460$ μm and $l_c = 410$ μm, respectively, at 1 THz. Including the effects of dispersion raises the coherence lengths of ZnTe and DAST to ~3 mm and 500 μm, respectively, at 1 THz as a result of resonances in the phonon bands of each of these crystals in the far IR. At 10 THz the polymer coherence length is expected still to be at least 500 μm, whereas at 10 THz the coherence lengths for ZnTe and DAST are 13 μm (Ref. 10) and <100 μm, respectively.[8] The result of these effects of increased coherence length and EO coefficient ($r_{33} \sim 100$ pm/V) is that EO polymers that generate THz fields that are ~3 orders of magnitude times that of ZnTe at 10 THz. The expected good phase-matching properties, large EO coefficients, and smooth films that should be possible with EO polymer composites provide the motivation for our studies of these materials.

In this Letter we describe the fabrication of EO polymer films and stacks made from these films and their subsequent use as generators and sensors of THz electromagnetic radiation. For each case, the

0146-9592/02/010055-03$15.00/0

polymer responses are directly compared with that from a 250-μm-thick $\langle 110 \rangle$ ZnTe crystal. We used a standard arrangement[21] to generate and detect the free-space propagation of THz waves. The laser was a regeneratively amplified Ti:sapphire laser (Coherent Mira/RegA 9000) that supplied $\sim$180 fs, 3–4 μJ, 795-nm optical pulses at 250 kHz. For comparison of the efficiency of EO polymers and ZnTe as THz emitters, we focused 90 mW of laser power to an elliptical spot of 6×10^{-4} cm^2 (150 W/cm^2). The ZnTe crystal was illuminated by p-polarized light at normal incidence, with the crystal rotated about the surface normal by 60° with respect to the $\langle \bar{1}10 \rangle$ direction to maximize the THz output. The polymer films were illuminated at an incident angle of 55° with p-polarized light. The detection was performed with crossed polarizers. For ZnTe, the normally incident probe beam was p polarized and the crystal was rotated about the $\langle 110 \rangle$ direction to maximize the detected signal. For the polymer, the probe beam was incident upon the polymer at 55° and was polarized at 45° with respect to the plane of incidence to maximize the overlap of the probe beam's polarization with the nonlinear optical coefficients of the poled polymer because the c axis of the poled polymer is normal to the surface of the film for the sandwich poling geometry.

The polymer films were guest–host mixtures of 25 wt. % dye molecule (3-(2-(4-(N,N-diethylamino)-phenyl)ethenyl)-5,5-dimethyl-1,2-cyclohexenylidene)-propanedinitrile (Lemke) and 75 wt. % poly(methyl methacrylate). The dye molecule[22] was obtained from Chromophore, Inc. The polymer was obtained from Aldrich Chemical. We made the films by dissolving each component in dichloroethane in a 10%/90% solid/solvent ratio and spreading the solution onto indium tin oxide- (ITO-) coated glass slides to allow the solvent to evaporate. Films 50–100 μm thick can easily be obtained in this fashion. The films are then baked at 85 °C to remove the solvent completely. After the films are baked, we make a sandwich from two polymer-coated slides by pressing the slides together in a vacuum oven at 250 °C for 10 min. Spacers of polyimide are placed between the slides to control the film thickness. A nonzero EO coefficient is imparted to the film by application of an electric field across the ITO electrodes in the sandwich while the sample temperature is held above the glass-transition temperature ($\sim$85 °C) of the composite. After cooling the films to room temperature, we measured the EO coefficients by the ellipsometric method.[23] Depending on the strength of the poling field, $r_{33} = 25$–33 pm/V for the various films. Before using the polymers in the THz setup, we removed one of the ITO slides from the sandwich. The film remained on one of the slides and was placed in the optical beam such that the THz beam did not transit the ITO layer.

Figure 1 compares the THz temporal signal and the corresponding frequency spectrum (inset) obtained from the EO polymer films and the 250-μm ZnTe used as emitters in conjunction with a 2-mm-thick ZnTe sensor. We obtained the multilayer films by removing the films completely from the ITO slides, laying them on top of the single-layer film (which remained attached to the glass slide), and holding the films together with clips. The THz amplitude obtained from the polymer increased with thickness, with $\sim$139-μm polymer thickness being equivalent to the 250-μm-thick ZnTe crystal. The spectrum is similar for both because of the presence of the 2-mm ZnTe sensor.

Figure 2 compares the THz temporal signal and its corresponding frequency spectrum (inset) obtained from the EO polymer films with the 250-μm ZnTe when these films are used as sensors in conjunction with a 2-mm–thick ZnTe emitter. Again, the spectra are similar and are dominated by the 2-mm ZnTe emitter. The double-layer polymer stack had an decreased signal-to-noise ratio. This is most likely caused by depolarization of the 795-nm sensor beam caused by the multiple polymer–air, polymer–ITO interfaces.

When they are used as emitters or sensors, the EO polymer films are more efficient than comparable thicknesses of ZnTe. The films used in this study had EO coefficients of 25–30 pm/V, but, because of

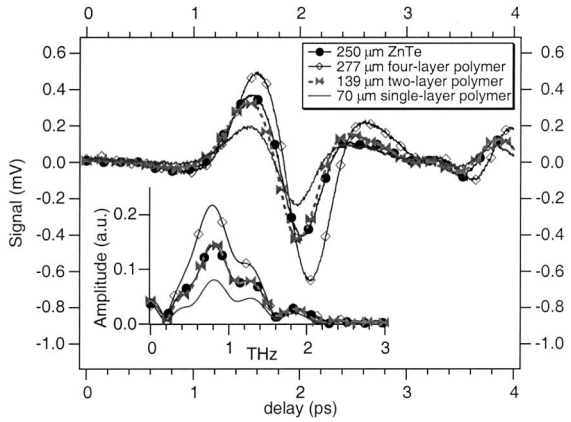

Fig. 1. Comparison of the THz field amplitudes and spectra (inset) obtained from four types of emitter. The signal from the 139-μm-thick two-layer polymer stack is virtually identical to the signal from the 250-μm ZnTe crystal. For each case the sensor was a 2-mm-thick crystal of $\langle 110 \rangle$ ZnTe.

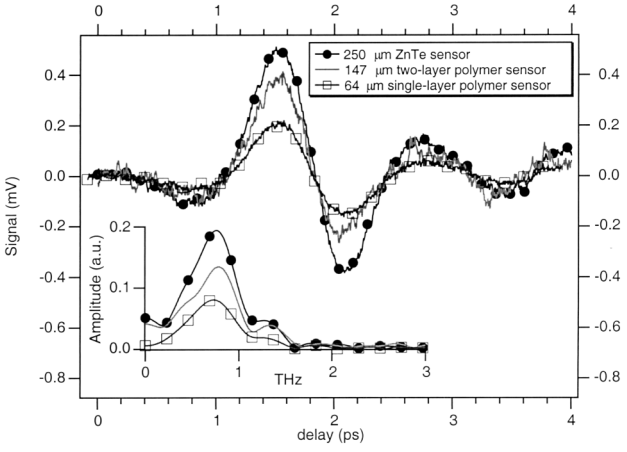

Fig. 2. Comparison of the THz field amplitudes and spectra (inset) obtained from three kinds of sensor. For each case the emitter was a 2-mm-thick crystal of $\langle 110 \rangle$ ZnTe.

the current poling geometry (sandwich), the potential of the polymer films is not fully realized. In-plane poling of the films would permit the use of normally incident pump and probe beams, giving rise to a much better overlap between the polarization of the optical beams and the poling axis. This geometry leads to an increase of a factor of ~1.7 in the effective EO coefficient compared with that for a film poled normally to the surface and used in a slanted geometry. We are currently developing an in-plane poling device for thick films and intend to report on those results elsewhere. Nevertheless, when we developed the sandwich technique we had in mind possible applications of these polymers in THz imaging for which large areas of poled material are necessary.

The use of polymers is not without its challenges, however. For example, because the glass-transition temperature of the current poly(methyl methacrylate)-based system is only 85 °C, r_{33} decays at room temperature to 75% of its original value in ~1 week. We can improve this decay rate by working with a polymer such as amorphous polycarbonate that has a higher glass-transition temperature. When the current dye molecule is placed in the amorphous polycarbonate matrix, we see a slight initial decay and then a leveling off of r_{33} at a value that is >90% of the original value, which has remained stable for nearly 2000 h now. Another potential problem with the use of organic materials is photodegradation. Continuous illumination of dye molecules with high-power lasers within or near the absorption band of the dye molecule will eventually lead to degradation of the dye molecule. When we continuously illuminated the current polymer composites ($\lambda_{max} = 510$ nm for Lemke) for 30 min with the 90-mW pump beam, we saw an 18% decrease in the emitted THz signal. This photodegradation is not significant for longer-wavelength pumps[17] such as those that emit at 1.3 μm.

Two other advantages of polymers compared with crystals are their mechanical properties and phase-matching characteristics. First, the ~70-μm-thick films used in this study are easy to make, flexible, easy to handle, and far cheaper than thin crystals of ZnTe. These properties should be useful in THz imaging applications because large-area polymer films can be made. The current films measure 1 cm × 1 cm. Second, because the dielectric constant of many polymers is in the range of 2–4 over the entire optical THz band, phase matching of the optical beam to the THz beam will be much better for the polymers than for the inorganic crystals,[15] resulting in better frequency response.

In summary, we have presented a new EO polymer material for THz applications and compared its performance with that of ZnTe. The polymer is easy enough to handle to permit stacking of the films for greater response and is inexpensive to fabricate. As these polymers should have relatively constant and low indices of refraction in the THz regime, which are approximately equal to the optical group velocities, we expect a significant improvement in bandwidth compared with that of ZnTe. Tests with 20-fs pulses are planned.

L. M. Hayden's e-mail address is hayden@umbc.edu.

References

1. M. C. Nuss and J. Orenstein, in *Millimeter and Submillimeter Wave Spectroscopy in Solids*, G. Grüner, ed., Vol. 74 of Topics in Applied Physics (Springer-Verlag, Berlin, 1998), pp. 7–50.
2. P. Y. Han, G. C. Cho, and X. C. Zhang, Opt. Lett. **25,** 242–244 (2000).
3. A. G. Markelz, A. Roitberg, and E. J. Heilweil, Chem. Phys. Lett. **320,** 42–48 (2000).
4. S. E. Ralph and D. Grischkowsky, Appl. Phys. Lett. **60,** 1070–1072 (1992).
5. S. Kono, M. Tani, and K. Sakai, in *Conference on Lasers and Electro-Optics (CLEO 2001)*, Vol. 56 of OSA Trends in Optics and Photonics Series (Optical Society of America, Washington, D.C., 2001), pp. 102–103.
6. S. Kono, M. Tani, and K. Sakai, Appl. Phys. Lett. **79,** 898–900 (2001).
7. P. Y. Han and X.-C. Zhang, Appl. Phys. Lett. **73,** 3049–3051 (1998).
8. P. Y. Han, M. Tani, F. Pan, and X.-C. Zhang, Opt. Lett. **25,** 675–677 (2000).
9. R. Huber, A. Brodschelm, F. Tauser, and A. Leitenstorfer, Appl. Phys. Lett. **76,** 3191–3193 (2000).
10. A. Nahata, A. Weling, and T. F. Heinz, Appl. Phys. Lett. **69,** 2321–2323 (1996).
11. X.-C. Zhang, Y. Lin, and X. F. Ma, Appl. Phys. Lett. **61,** 2764–2766 (1992).
12. A. Rice, Y. Jin, X. F. Ma, X.-C. Zhang, D. Bliss, J. Larkin, and M. Alexander, Appl. Phys. Lett. **64,** 1324–1326 (1994).
13. A. Bonvalet, M. Joffre, J. L. Martin, and A. Migus, Appl. Phys. Lett. **67,** 2907–2909 (1995).
14. T. J. Carrig, G. Rodriguez, T. S. Clement, A. J. Taylor, and K. R. Stewart, Appl. Phys. Lett. **66,** 121–123 (1995).
15. A. Nahata, D. Auston, C. Wu, and J. T. Yardley, Appl. Phys. Lett. **67,** 1358–1360 (1995).
16. A. Nahata, D. H. Auston, T. F. Heinz, and C. Wu, Appl. Phys. Lett. **68,** 150–152 (1996).
17. Y. Shi, C. Zhang, H. Zhang, J. H. Bechtel, L. R. Dalton, B. H. Robinson, and W. H. Steier, Science **288,** 119–122 (2000).
18. F. Pan, G. Knöpfle, C. Bosshard, S. Follonier, R. Spreiter, M. S. Wong, and P. Günter, Appl. Phys. Lett. **69,** 13–15 (1996).
19. M.-C. Oh, H. Zhang, A. Szep, V. Chuyanov, W. H. Steier, C. Zhang, L. R. Dalton, H. Erlig, B. Tsap, and H. Fetterman, Appl. Phys. Lett. **76,** 3525–3527 (2000).
20. A. Nahata and T. F. Heinz, in *Ultrafast Electronics and Optoelectronics*, M. C. Nuss and J. Bowers, eds., Vol. 13 of OSA Trends in Optics and Photonics Series (Optical Society of America, Washington, D.C., 1997), pp. 218–221.
21. Z. Jiang and X. C. Zhang, IEEE Trans. Microwave Theory Tech. **47,** 2644–2650 (1999).
22. R. Lemke, Chem. Ber. **103,** 1894–1895 (1970).
23. Sandalphon, B. Kippelen, K. Meerholz, and N. Peyghambarian, Appl. Opt. **35,** 2346–2354 (1996).